Asian Journal of Chemistry; Vol. 36, No. 9 (2024), 2013-2018

ASIAN JOURNAL OF CHEMISTRY

https://doi.org/10.14233/ajchem.2024.31999

Exploring the Third-Order Non-linear Optical Responses and Optical Limiting Properties of *p*-Nitroaniline Picrate: A Theoretical and Experimental Study

ANJU LINDA VARGHESE[1,*], P.L. MARIA LINSHA[2] and GEORGE MATHAI[3]

[1]Department of Chemistry & Centre for Research, Baselius College, Kottayam-686001, India
[2]Department of Chemistry, St. Teresa's College (Autonomous), Kochi-682031, India
[3]Department of Chemistry, Sacred Heart College, Thevara-682013, India

*Corresponding author: E-mail: lindaanju@gmail.com

Received: 23 May 2024; *Accepted*: 29 June 2024; *Published online*: 30 August 2024; AJC-21725

The current study investigates the nonlinear optical behaviour of *p*-nitroaniline picrate, which has been synthesized and characterized. Its third-order non-linear optical properties were investigated *via* Z-scan studies. *p*-Nitroaniline picrate demonstrates a reverse saturable absorption, as indicated by a positive absorption coefficient (b), which is of the order 10^{-12} m/W. Closed aperture data indicate a positive refractive non-linearity due to self-focusing, with non-linear refractive index (n_2), third-order susceptibility ($\chi^{(3)}$) and second-order hyperpolarizability (g) in order of 10^{-19} m^2/W, 10^{-13} esu and 10^{-34} esu, respectively. Theoretical calculations corroborated the experimental findings, emphasizing the significant third-order non-linearities of *p*-nitroaniline picrate. An optical limiting property is demonstrated with a threshold of 16.32 J/cm^2. Low HOMO-LUMO energy gaps, intermolecular hydrogen bonding and intramolecular charge transfer interactions are the properties that are related to these qualities according to DFT research. Therefore, *p*-nitroaniline picrate is highly recommended for the optical limiting applications.

Keywords: *p*-Nitroaniline picrate, Third-order, Non-linear optical (NLO) properties, Optical limiting.

INTRODUCTION

Non-linear optics is a branch of optics which explores the interactions of light with materials, where the optical properties of the material vary non-linearly with the intensity of light [1,2]. Third-order optical non-linearities are particularly significant, involving processes such as third-harmonic generation, self-phase modulation and optical Kerr effect [3-6]. These non-linear phenomena are crucial for various applications, including the optical signal processing, frequency conversion and optical limiting [7-9]. Optical limiting is particularly significant as it involves the control or mitigation of intense light sources, such as lasers, to prevent damage or disruption to sensitive optical components or human eyesight, making it indispensable in laser safety, defense technologies and telecommunications [10,11].

Organic molecules containing aromatic rings hold considerable promise for both second and third-order non-linear optical applications due to their remarkable non-linearity, high optical damage threshold and rapid electronic response [12]. Among these, picric acid derivatives are particularly intriguing candidates, as they have charge transfer interactions readily, since picrates exhibit strong non-linear optical (NLO) activity [13-16]. Nevertheless, the NLO properties of *p*-nitroaniline picrate have not been extensively studied. Thus, this study aims to investigate comprehensively the third-order non-linear optical responses and optical limiting properties of *p*-nitroaniline picrate through the theoretical modeling as well as by experimental analysis, with the ultimate goal of advancing its potential for non-linear device applications.

EXPERIMENTAL

The reagents and chemical used for the synthesis were of AR grade. Solvents were purified and dried according to standard procedures. *p*-Nitroaniline and picric acid were purchased from Merck and used without further purification. Purity of the product was checked by TLC and melting point determination (Buchi, B540). Characterization was done using FT-IR (Bruker Alpha-E FT IR).

Synthesis of *p*-nitroaniline picrate: *p*-Nitroaniline picrate was synthesized by slow evaporation of methanolic solution containing equimolar amount of *p*-nitroaniline and picric acid [17]. Solution of equimolar amounts of *p*-nitroaniline and picric acid in methanol were prepared separately by dissolving 1.2 g of *p*-nitroaniline in 15 mL ethanol and 2.2 g picric acid in 30 mL ethanol. After mixing the two solutions, the resultant solution was stirred well. Within 2 days, bright red crystals of *p*- nitroaniline picrate were formed. It was then filtered off, dried and repeatedly recrystallized from pure methanol to enhance the purity of salt (**Scheme-I**). Purity was checked by TLC and melting point determination. Melting point for the picrate was obtained as 167.6 ºC (methanol).

Z-scan studies: The Z-scan technique was employed to study the third-order non-linear optical properties of *p*-nitroaniline picrate, offering an effective and accurate means to measure non-linear absorption, non-linear refraction and third-order non-linear optical susceptibility of materials [18,19]. In this technique, the sample is traversed along the focal point of the lens, with non-linear absorption stemming from either two-photon absorption or multiphoton absorption mechanisms within the compound. Reverse saturable absorption (RSA) arises from two-photon absorption, while saturable absorption (SA) results from multiphoton absorption. Furthermore, the self-focusing or self-defocusing of the sample is closely connected to its non-linear refraction, which offers valuable understanding of the material's sign of non-linear refraction. In order to possess the optical limiting property, a molecule must display both reverse saturable absorption behaviour and positive non-linear refractive characteristics.

Z-scan measurement was carried out using Q-switched Nd-YAG laser having 5 ns pulses at a repletion rate of 10 Hz giving second harmonic at 532 nm. The laser beam was focused by a lens of 10 cm focal length. In this technique, sample was mounted on the translation stage and translating the sample between +Z and –Z position along Z-direction. The radius of the beam waist ω_0 was calculated to be 35 μm. The Rayleigh length, $z_0 = \frac{\pi\omega_0^2}{\lambda}$ was calculated as 7.42 mm, is greater than the thickness of the sample cuvette (1 mm), an essential requirement for Z-scan experiments [20].

The third- order non-linear refractive index (n_2) and non-linear absorption coefficient (β), third order NLO susceptibility ($\chi^{(3)}$), second hyperpolarizability (g) (third order effect) of *p*-nitroaniline picrate in acetone having 0.5 mM concentration and intensity at 1.08 GW/cm^2 were evaluated by closed and open aperture Z-scan techniques.

Computational details: Gaussian 09 for windows software package was used for DFT calculation. The B3LYP hybrid functional has proven to be reliable for calculating the geometrical parameters, electronic and vibrational wavenumbers [21]. The ground state structure was optimized and frequency calculations were performed to ensure that the optimized structure is minimum in the potential energy surface using B3LYP/6-31G (d,p) level. Second hyperpolarizability (g) for the studied compound was calculated by DFT approach using CAM-B3LYP/6-31G(d,p), which is currently one of the ultimate procedures for obtaining numerically accurate NLO responses [22,23]. GaussView 5 for windows software was used for generating the input files and visualization of the results.

RESULTS AND DISCUSSION

FT-IR studies: FT- IR spectrum of *p*-nitroaniline picrate (Fig. 1) shows a characteristic band at 3580 cm^{-1} due to the O-H stretching vibrations. The N-H stretching vibrations of the amino group appear at 3377 and 3486 cm^{-1}, while aromatic ring C-H stretching vibrations are observed at 3090 cm^{-1}. An intense band at 1620 cm^{-1} is assigned to N-H bending vibrations and the aromatic ring skeletal vibrations are detected at 1451 cm^{-1}. The nitro group exhibits an asymmetric stretching vibration at 1493 cm^{-1} and a symmetric stretching vibration at 1346 cm^{-1}. Additionally, the phenolic C-O stretching vibration occurs at 1248 cm^{-1} and the aromatic ring C-H bending vibrations are indicated at 919 and 750 cm^{-1}.

Third order non-linear optical studies of *p*-nitroaniline picrate

Open aperture (OA) Z-scan plot: Non-linear absorption characteristics of *p*-nitroaniline picrate have been obtained from open aperture Z-scan plot. Fig. 2 shows the open aperture (OA) Z-scan curve of *p*-nitroaniline picrate at 0.5 mM concentration in acetone and 1.08 GW/cm^2 intensity. The obtained OA curve shows reverse saturation behaviour, hence the absorption coefficient β is positive. A material with reverse saturable absorption property shows increase in absorption when increase in laser intensity. From the curve, it is clear that open aperture plot of *p*-nitroaniline picrate shows excellent agreement with theoretical studies.

Closed aperture (CA) Z-scan plot: The non-linear refractive index of *p*-nitroaniline picrate has been investigated by closed aperture Z-scan technique. The closed aperture (CA) Z-scan plot at 0.5 mM concentration in acetone and 1.08 GW/cm^2 intensity have been recorded and shown in Fig. 3. The valley followed by a peak in the normalized transmittance obtained

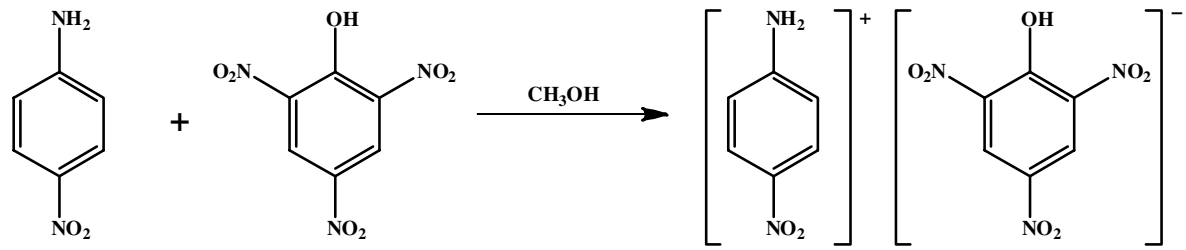

Scheme-I: Synthesis of *p*-nitroaniline picrate

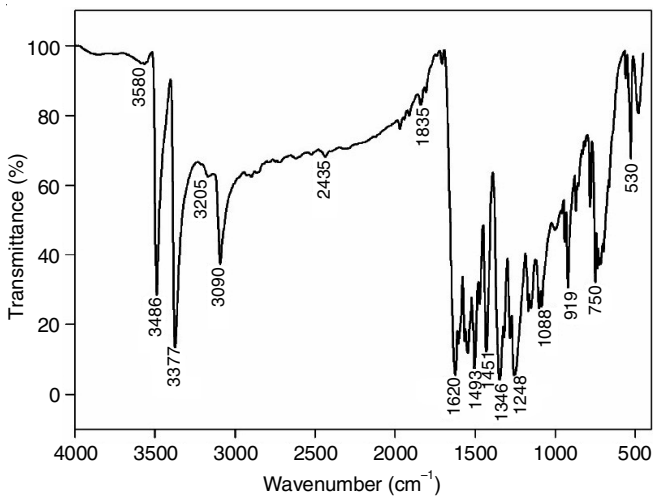

Fig. 1. FT-IR spectrum of *p*-nitroaniline picrate

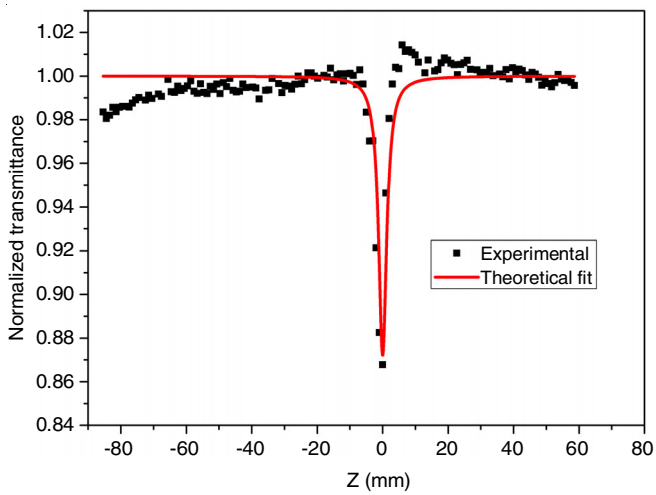

Fig. 2. Open aperture (OA) Z-scan plot of *p*-nitroaniline picrate

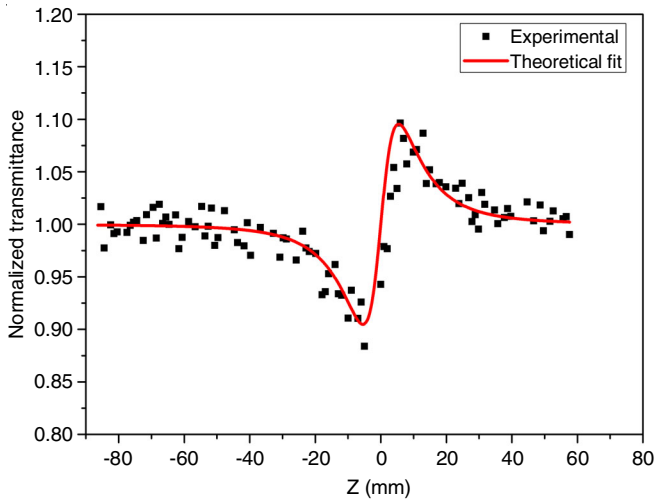

Fig. 3. Closed aperture (CA) Z-scan plot of *p*-nitroaniline picrate

from the closed aperture data of *p*-nitroaniline picrate indicated that the sign of the refractive non-linearity is positive due to self-focusing. Pure non-linear refraction curves were obtained by division of closed aperture data by open aperture data.

The normalized transmittance T(z) is given by

$$T(z,\Delta\phi_0) = 1 - \frac{4\Delta\phi_0 x}{(x^2+9)(x^2+1)} \quad (1)$$

where $\Delta\phi_0$ is the on axis non-linear phase shift and x is z/z_0. The non-linear refractive index (n_2) and real part of third-order non-linear susceptibility, $Re\chi^{(3)}$ were calculated by the following relations [20]:

$$n_2 = \frac{\Delta\phi_0\lambda}{2\pi I_0 L_{eff}} \quad (2)$$

$$Re\,\chi^{(3)} = 10^{-4}\frac{\varepsilon_0 n_0^2 c^2}{\pi} n_2 \quad (3)$$

The imaginary part of the third order susceptibility ($Im\chi^{(3)}$) was calculated from β through the relation (eqn. 4):

$$Im\,\chi^{(3)} = 10^{-2}\frac{\varepsilon_0 n_0^2 c^2 \lambda}{4\pi^2}\beta \quad (4)$$

where ε_0 is the permittivity of free space, c is the velocity of light in vacuum and n_0 is the linear refractive index.

The third-order non-linear susceptibility ($\chi^{(3)}$) was calculated from the relation (eqn. 5):

$$\chi^{(3)} = \left[(Re\chi^{(3)})^2\right] + \left[(Im\chi^{(3)})^2\right]^{1/2} \quad (5)$$

The second order hyperpolarizability, γ of the sample is related to the third-order susceptibility through eqn. 6:

$$\gamma = \frac{\chi^{(3)}}{\left[\frac{1}{3}\left(n_0^2+2\right)\right]^4 N} \quad (6)$$

where N is the molecular number density in cm^{-3}.

The third order non-linear refractive index (n_2), non-linear absorption coefficient (β), third order NLO susceptibility ($\chi^{(3)}$) and second order hyperpolarizability (γ) of *p*-nitroaniline picrate in acetone having 0.5 mM concentration and intensity at 1.08 GW/cm^2 were evaluated by the measurements of closed and open aperture Z-scan techniques and are listed in Table-1.

The values presented in Table-1 highlight key non-linear optical properties of the material under study, which have significant implications for various applications in photonics and optoelectronics. The non-linear absorption coefficient β (m/w) is of the order of 10^{-12} indicates the material's ability to absorb light in a manner dependent on the light intensity, which is crucial for applications such as optical limiting and protection of sensitive optical components from high-intensity light. The non-linear refractive index (n_2) is of the order 10^{-19} m^2/W, which measures the intensity-dependent change in the refractive index,

TABLE-1
THIRD-ORDER NON-LINEAR OPTICAL PARAMETERS OF *p*-NITROANILINE PICRATE

β (× 10^{-12}) (m/W)	n_2 (× 10^{-19}) (m^2/W)	Re $\chi^{(3)}$ (× 10^{-13}) (esu)	Im $\chi^{(3)}$ (× 10^{-13}) (esu)	$\chi^{(3)}$ (× 10^{-13}) (esu)	γ (× 10^{-34} esu)
4.4019	5.6904	4.5972	1.5733	4.8589	7.2406

essential for applications in all-optical switching, modulation and the development of advanced photonic devices that leverage light. The non-linear refractive index $\chi^{(3)}$ and γ are of the order of 10^{-13} esu and 10^{-34} esu, respectively. The $\chi^{(3)}$ is a fundamental parameter describing the third-order non-linear response of the material, whereas γ further elucidates the strength of the non-linear interaction, providing insights into the efficiency of various non-linear optical processes in the material.

Optical limiting properties: Fig. 4 shows the optical limiting curve of *p*-nitroaniline picrate where the normalized transmission is plotted as a function of input power for 0.5 mM solution. At a certain threshold value, *i.e.* 16.32 J/cm^2 self focusing effect occurs, which reduces the proportional intensity of beam passing the detector. Thus, the transmittance recorded by the detector reduced considerably. The relevance of this finding lies in its potential application in optical limiting devices, which are crucial for protecting sensitive optical sensors and human eyes from damage caused by high-intensity light sources. The self-focusing phenomenon, which effectively clamps the transmitted intensity, makes *p*-nitroaniline picrate an attractive candidate for developing advanced optical limiters.

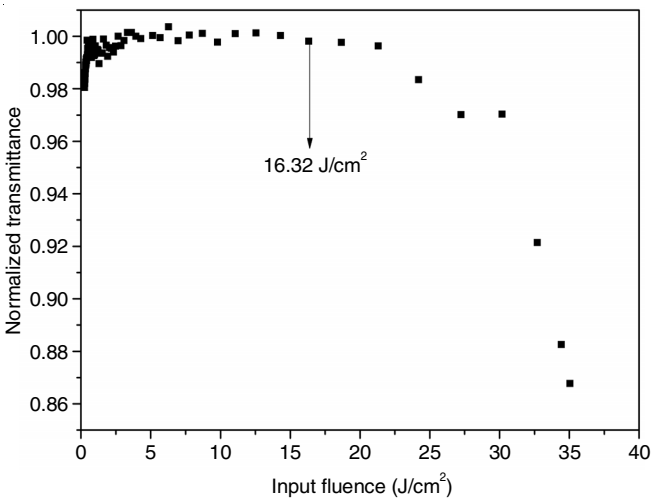

Fig. 4. Optical limiting curve of *p*-nitroaniline picrate

DFT studies

Geometry optimization: Ground state structure of *p*-nitroaniline picrate was optimized using B3LYP/6-31G (d, p) level and is given in Fig. 5. Selected dihedral angles obtained from DFT method are tabulated in Table-2 and confirmed the planar π-conjugation. From the optimized geometry, the dihedral angles C_2-C_1-N_{15}-O_{17} (32.49º), C_2-C_1-N_{15}-O_{16} (-145.525º), C_4-C_5-N_{12}-O_{13} (151.3º) and C_4-C_5-N_{12}-O_{14} (-30.3º) show that the nitro groups (N_{12} and N_{15}) are slightly tilted from the ring. This is due to the common tendency of the *o*-nitro groups to be out of plane in the picrate anion explained as a result of repulsion between the phenolate and nitro-oxygen atoms and the simultaneous attraction of a partially positively charged nitrogen atom, thereby, no possibility of intramolecular hydrogen bonding. The hydrogen bond distance O_{18}-H_{19}---N_{20} (2.146 Å) and OHN angle is (132.11º) within the hydrogen bond limit, which shows the O-H—N intermolecular hydrogen bonding.

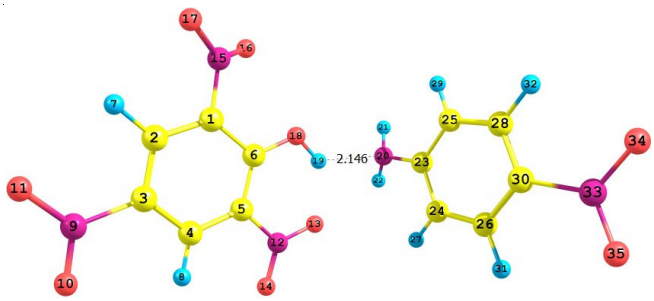

Fig. 5. Optimized geometry of *p*-nitroaniline picrate

TABLE-2
SELECTED DIHEDRAL ANGLES OF *p*-NITROANILINE PICRATE

Dihedral angles	Value (°)	Dihedral angles	Value (°)
C_1-C_2-C_3-C_4	1.084	H_7-C_2-C_3-C_4	1.733
C_2-C_3-C_4-C_5	0.233	H_8-C_4-C_5-O_{12}	-0.064
C_3-C_4-C_5-C_6	-0.615	C_{23}-C_{24}-C_{26}-C_{30}	0.201
C_4-C_5-C_6-C_1	-0.299	C_{24}-C_{26}-C_{30}-C_{28}	0.096
N_{15}-C_1-C_6-O_{18}	3.746	C_{26}-C_{30}-C_{28}-C_{25}	-0.179
N_{15}-C_1-C_6-H_7	-2.281	C_{23}-C_{25}-C_{28}-C_{30}	-0.036

Frontier molecular orbitals (FMOs): HOMO and LUMO orbitals for *p*-nitroaniline picrate obtained using B3LYP functionals and 6-31G(d, p) basis set are shown in Fig. 6. Electron population analysis reveals that HOMO extends over *p*-nitroaniline donor moiety, whereas LUMO resides over picric acid part. Hence, probable electron flow should be from *p*-nitroaniline donor to picric acid acceptor, which are bonded through

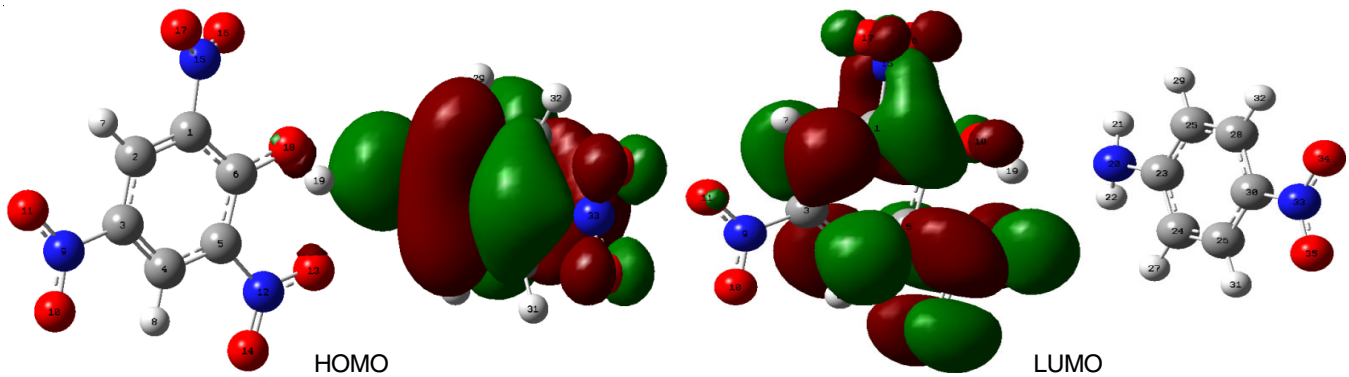

Fig. 6. Frontier molecular orbitals of *p*-nitroaniline picrate

intermolecular hydrogen bonding. Energies of HOMO-LUMO and energy gaps of *p*-nitroaniline picrate are listed in Table-3.

TABLE-3
ENERGIES OF HOMO-LUMO AND ENERGY GAPS OF *p*-NITROANILINE PICRATE

Energy of HOMO (Hartrees)	Energy of HOMO (Hartrees)	HOMO-LUMO energy gap	
		in Hartrees	in eV
-0.2216	-0.1119	0.1097	2.9851

The small energy gap between the HOMO and LUMO in *p*-nitroaniline picrate facilitates easier electron transfer. This enhanced electron mobility leads to a stronger non-linear optical (NLO) response, as the material can more readily undergo polarization in response to an applied optical field. Consequently, this property enhances the efficiency of processes such as second harmonic generation and other NLO phenomena, making *p*-nitroaniline picrate more effective for applications in photonics and optoelectronics.

Natural bond orbital analysis: Natural bond orbital (NBO) is proved to be an effective tool for chemical interpretation of hyperconjugative interaction and electron density transfer from the filled lone pair electron [24]. The hyperconjugative interaction energy E(2), deduced from the second-order perturbation approach.

$$E(2) = \Delta E_{ij} = q_i \frac{F(i,j)^2}{\varepsilon_j - \varepsilon_i} \quad (7)$$

where q_i is the donor orbital occupancy, ε_i, ε_j are the diagonal elements (orbital energies) and F(i,j) is the off-diagonal NBO Fock matrix element.

The NBO analysis has been performed on *p*-nitroaniline picrate to identify and explain the formation of the intermolecular hydrogen bonding between picric acid and *p*-nitroaniline and also to elucidate the intramolecular charge transfer interaction. The calculated values for some prominent interactions are shown in Table-4.

Strong intramolecular hyperconjugative interaction is also observed in *p*-nitroaniline picrate. Stabilization energy E(2) associated with hyperconjugative interaction of $\sigma(O_{12}\text{-}H_{19})$ and $\sigma^*(N_{20}\text{-}H_{21})$ was obtained as 693.5 kJ/mol. Hydrogen bonding interaction leads to an increase in electron density of N-H antibonding orbital. Electron density on $\sigma^*(N_{12}\text{-}H_{13})$ is 0.57969 e. This increase of population in NH antibonding orbital weakens the N-H bond, which is an indicative of intermolecular hydrogen bonding. The intramolecular hyperconjugative interactions are formed by the orbital overlap between π(C-C) and π^*(C-C) bond orbitals, which results intramolecular charge transfer causing stabilization of the system. These interactions are observed as an increase in electron density in π^*(C-C) orbital that weakens the respective bonds. The electron density at the conjugated π-bonds (1.65-1.75 e) and π^* bonds (~0.21-0.41 e) clearly demonstrates charge delocalization of electron leading to stabilization energy ~80-260 kJ/mol.

DFT studies on the second order hyperpolarizabilities: Second order hyperpolarizability (γ) of *p*-nitroaniline picrate has been evaluated theoretically at CAM B3LYP/6-31G(d,p) level using eqn. 8. For the calculations in solution phase, CPCM model was employed which is part of Gaussian 09.

$$\langle\gamma\rangle = \frac{1}{5}\left[\gamma_{xxxx} + \gamma_{yyyy} + \gamma_{zzzz} + 2(\gamma_{xxyy} + \gamma_{xxzz} + \gamma_{yyzz}\right] \quad (8)$$

Relevant second order hyperpolarizability components and calculated g value has been tabulated in Table-5. The calculated g value is of the order 10^{-34} esu which are in good agreement with experimental value (7.2406×10^{-34} esu).

Conclusion

p-Nitroaniline picrate was synthesized and characterized and found to be third order NLO active from Z-scan study. The Z-scan technique reveals its reverse saturation behaviour,

TABLE-4
NATURAL BOND ORBITAL ANALYSIS OF *p*-NITROANILINE PICRATE

Donor (i)	ED (e)	Acceptor (j)	ED (e)	E(2)[a] (kJmol^{-1})	E(i)–E(j)[b] (kJ mol^{-1})	F(i,j)[c] (kJ mol^{-1})
Within unit 1						
$\pi(C_1\text{-}C_6)$	1.67536	$\pi^*(C_4\text{-}C_5)$	0.39548	185.03	39230.64	160.15
$\pi(C_1\text{-}C_6)$	1.67536	$\pi^*(C_2\text{-}C_3)$	0.21726	147.43	44943.84	149.65
$\pi(C_3\text{-}C_4)$	1.72364	$\pi^*(C_5\text{-}C_6)$	0.32638	165.77	4951.44	223.16
$\pi(C_1\text{-}C_2)$	1.75638	$\pi^*(N_{15}\text{-}O_{17})$	0.29816	288.86	6094.08	288.80
$\pi(C_3\text{-}C_4)$	1.72364	$\pi^*(N_9\text{-}O_{10})$	0.65454	3089.88	380.88	238.92
$\pi(C_4\text{-}C_5)$	1.79364	$\pi^*(N_{12}\text{-}O_{14})$	0.55454	331.33	6094.08	328.18
LP (2)O_{13}	1.46709	$\pi^*(N_{12}\text{-}O_{14})$	0.55454	663.54	367.56	359.69
LP (2)O_{16}	1.46709	$\pi^*(N_{15}\text{-}O_{17})$	0.39548	448.367	22471.92	194.28
From unit 1 to unit 2						
$\sigma(O_{12}\text{-}H_{19})$	1.58865	$\sigma^*(N_{20}\text{-}H_{21})$	0.57969	693.50	2028.34	247.12
Within unit 2						
$\pi(C_{23}\text{-}C_{25})$	1.68276	$\pi^*(C_{24}\text{-}C_{26})$	0.38344	254.42	367.56	252.04
$\pi(C_{23}\text{-}C_{25})$	1.68276	$\pi^*(C_{28}\text{-}C_{30})$	0.41311	260.62	367.56	217.91
$\pi(C_{23}\text{-}C_{25})$	1.68276	$\sigma^*(N_{20}\text{-}H_{21})$	0.59967	82.09	498.84	152.27
$\pi(C_{26}\text{-}C_{30})$	1.66323	$\pi^*(C_{25}\text{-}C_{28})$	0.38344	253.63	367.56	254.67
$\pi(C_{26}\text{-}C_{30})$	1.66323	$\pi^*(C_{23}\text{-}C_{24})$	0.45311	158.61	367.56	267.91
$\pi(C_{26}\text{-}C_{30})$	1.66323	$\pi^*(N_{33}\text{-}O_{35})$	0.59503	117.40	420.07	168.03
LP (2) O_{34}	1.46258	$\pi^*(N_{33}\text{-}O_{35})$	0.62053	647.55	393.82	359.69

TABLE-5
SECOND ORDER HYPERPOLARIZABILITY COMPONENTS AND RESULTANT VALUES OF γ

$\gamma_{xxxx} \times 10^{-34}$ esu	$\gamma_{yyyy} \times 10^{-34}$ esu	$\gamma_{zzzz} \times 10^{-34}$ esu	$\gamma_{xxyy} \times 10^{-34}$ esu	$\gamma_{xxzz} \times 10^{-34}$ esu	$\gamma_{yyzz} \times 10^{-34}$ esu	$<\gamma> \times 10^{-34}$ esu
17.980	-17.732	-7.248	22.566	1.448	-1.616	7.937

characterized by a positive absorption coefficient (β) of the order 10^{-12} m/W. This behaviour is crucial for optical limiting, which protects sensitive optical sensors from damage by intense light pulses. The positive non-linear refractive index (n_2) of the order 10^{-19} m^2/W indicating the self-focusing properties, essential for beam control in optical systems. The third-order non-linear optical susceptibility ($\chi^{(3)}$) and the second-order hyperpolarizability (γ) are of the order of 10^{-13} esu and 10^{-34} esu, respectively, confirm the strong non-linear response of picrate. Theoretical calculations using the CAM-B3LYP/6-31G (d,p) method corroborate these experimental findings, emphasizing the reliability of the data. The optical limiting threshold of 16.32 J/cm^2 indicates its effectiveness in limiting high-intensity light, ensuring its applicability in protecting optical devices. These properties highlight the potential of *p*-nitroaniline picrate in optical limiting applications, where the controlling light intensity is crucial for device safety and performance. The DFT calculations were employed to find out the structural and electronic factors, which contribute to its NLO behaviour. The low HOMO-LUMO of energy gap facilitates efficient intramolecular charge transfer, enhancing its non-linear optical properties. NBO analysis reveals the existence of intermolecular hydrogen bonding and intramolecular charge transfer interactions which contribute to the significant polarization within *p*-nitroaniline picrate molecules, further enhancing its NLO performance. Therefore, *p*-nitroaniline picrate is highly recommended for use in optical limiting applications, given its robust third-order NLO characteristics and practical optical limiting capabilities.

ACKNOWLEDGEMENTS

Department of Physics, Mar Ivanios College (Autonomous), Thiruvananthapuram is deeply acknowledged for their invaluable expertise in conducting Z-Scan studies and Optical Limiting investigations of our molecule.

CONFLICT OF INTEREST

The authors declare that there is no conflict of interests regarding the publication of this article.

REFERENCES

1. S. Ahmed, X. Jiang, C. Wang, U.E. Kalsoom, B. Wang, Y. Muhammad, J. Khan, Y. Duan, H. Zhu, X. Ren and H. Zhang, *Adv. Opt. Mater.*, **9**, 2001671 (2021); https://doi.org/10.1002/adom.202001671
2. N.C. Panoiu, W.E.I. Sha, D.Y. Lei and G.-C. Li, *J. Opt.*, **20**, 083001 (2018); https://doi.org/10.1088/2040-8986/aac8ed
3. S. Khorasani, *Commum. Theor. Phys.*, **70**, 344 (2018); https://doi.org/10.1088/0253-6102/70/3/344
4. L. Sirleto and G.C. Righini, *Micromachines*, **14**, 604 (2023); https://doi.org/10.3390/mi14030604
5. G. Lin and Q. Song, *Laser Photonics Rev.*, **16**, 2100184 (2022); https://doi.org/10.1002/lpor.202100184
6. M. Li, C.-L. Zou, C.-H. Dong and D.-X. Dai, *Opt. Express*, **26**, 27294 (2018); https://doi.org/10.1364/OE.26.027294
7. B. Gu, C. Zhao, A. Baev, K.-T. Yong, S. Wen and P.N. Prasad, *Adv. Opt. Photonics*, **8**, 328 (2016); https://doi.org/10.1364/AOP.8.000328
8. S.K. Turitsyn, J.E. Prilepsky, S.T. Le, S. Wahls, L.L. Frumin, M. Kamalian and S.A. Derevyanko, *Optica*, **4**, 307 (2017); https://doi.org/10.1364/OPTICA.4.000307
9. Y. Song, Y. Chen, X. Jiang, W. Liang, K. Wang, Z. Liang, Y. Ge, F. Zhang, L. Wu, J. Zheng, J. Ji and H. Zhang, *Adv. Opt. Mater.*, **6**, 1701287 (2018); https://doi.org/10.1002/adom.201701287
10. E. Mathew, V.V. Salian, B. Narayana and I.H. Joe, *J. Mol. Struct.*, **1250**, 131704 (2022); https://doi.org/10.1016/j.molstruc.2021.131704
11. D. Dini, M.J.F. Calvete and M. Hanack, *Chem. Rev.*, **116**, 13043 (2016); https://doi.org/10.1021/acs.chemrev.6b00033
12. S. Nandhini and P. Murugakoothan, *Opt. Mater.*, **113**, 110714 (2021); https://doi.org/10.1016/j.optmat.2020.110714
13. D. Arthi, E. Ilango, M. Mercina, D. Jayaraman and V. Joseph, *J. Mol. Struct.*, **1127**, 156 (2017); https://doi.org/10.1016/j.molstruc.2016.07.030
14. R.O.M.U. Jauhar, V. Viswanathan, P. Vivek, G. Vinitha, D. Velmurugan and P. Murugakoothan, *RSC Adv.*, **6**, 57977 (2016); https://doi.org/10.1039/C6RA10477K
15. P. Karthiga Devi and K. Venkatachalam, *J. Mater. Sci. Mater. Electron.*, **27**, 8590 (2016); https://doi.org/10.1007/s10854-016-4877-7
16. E. Shobhana, B. Balraj, M. Bharathi and V. Sathyanarayanamoorthi, *Asian J. Chem.*, **35**, 2603 (2023); https://doi.org/10.14233/ajchem.2023.28258
17. P.K. Sivakumar, M.K. Kumar, R.M. Kumar and R. Kanagadurai, *Mod. Phys. Lett. B*, **27**, 1350235 (2013); https://doi.org/10.1142/S0217984913502357
18. S.S. Thakare, M.C. Sreenath, S. Chitrambalam, I.H. Joe and N. Sekar, *Opt. Mater.*, **64**, 453 (2017); https://doi.org/10.1016/j.optmat.2017.01.020
19. M.C. Sreenath, I. Hubert Joe and V.K. Rastogi, *Opt. Laser Technol.*, **108**, 218 (2018); https://doi.org/10.1016/j.optlastec.2018.06.056
20. J.S.-D. Tovar, S. Valbuena-Duarte and F. Racedo-Niebles, *Rev. Fac. Ingenieria*, **86**, 27 (2018); https://doi.org/10.17533/udea.redin.n86a04
21. Y.S. Mary, H.T. Varghese, C.Y. Panicker, M. Girisha, B.K. Sagar, H.S. Yathirajan, A.A. Al-Saadi and C. Van Alsenoy, *Spectrochim. Acta A Mol. Biomol. Spectrosc.*, **150**, 543 (2015); https://doi.org/10.1016/j.saa.2015.05.090
22. A. Linda Varghese, I. Abraham and M. George, *Mater. Today Proc.*, **9**, 92 (2019); https://doi.org/10.1016/j.matpr.2019.02.041
23. N. Andijani and N.A. Wazzan, *Results Phys.*, **11**, 605 (2018); https://doi.org/10.1016/j.rinp.2018.10.002
24. B.K. Paul and N. Guchhait, *Comput. Theor. Chem.*, **972**, 1 (2011); https://doi.org/10.1016/j.comptc.2011.06.004